Algorithm Theoretical Basis Document (ATBD)

MERIS Regional Case 2 Water BEAM Extension

Performance of the Atmospheric Correction

Part: Sun Glint Correction

Version 0.8, 23. July 2006

Roland Doerffer & Helmut Schiller

GKSS Forschungszentrum Geesthacht GmbH

21502 Geesthacht

ESRIN Contract: No. 18639/04/I-LG

MERIS Case 2 Water Algorithms Development

Distribution

Name:

P. Regner (ESA / ESRIN)

C. Brockmann (BC)

Change Record

Issue	Revision	Date	Description
Draft 0.1	0	24.10.2005	Initial draft
Draft 0.8	1	23.8.2006	Draft
Final Version 1.0	tbc	tbc	Final Version

Abstract

1 Preface

This report describes the performance of the atmospheric correction procedure as implemented in version 0.7 of the MERIS Case 2 water BEAM plug-in, which has been developed under contract of the European Space Agency by GKSS and Brockmann Consult.

2 Document History

This is the first version of the document.

3 Introduction

The determination of water leaving radiance reflectances from top of atmosphere radiance reflectances (shortly called "atmospheric correction") is the most critical step in ocean colour remote sensing, since the atmospheric path radiance can surmount the water leaving radiance by a factor of 10. A particular problem exists over coastal waters for a number of reasons:

1. High suspended matter concentrations cause also a significant contribution to the water leaving radiance in the near infrared bands, which under case 1 water conditions are normally used for determining the atmospheric path radiance due to the high absorption of pure water. Thus, for turbid water cases there are no longer spectral bands available, which are independent from the influence of water constituents.

2. In some areas, such as the Baltic Sea, cyanobacteria can float in form of blooms very close or on the water surface, so that the problem of getting the path radiance from NIR bands becomes even more difficult.

3. Waters with high concentrations of yellow substances and / or phytoplankton pigments have a very low reflectance in the blue spectral bands. Thus, in contrast to most case 1 water conditions, the signal is so low that small errors in the determination of the path radiance, which is determined from extrapolation from the NIR bands, lead to wrong, often negative reflectances in this spectral range.

4. In coastal zones many different aerosols may occur due to industrial emissions or desert dust blowing into the sea. Thus, a treatment of such a complex and varying mixture of different aerosols may not be possible in one algorithm. Furthermore, contrails by dense aircraft traffic in the vicinity of flight routes and / or airports may cause severe problems in atmospheric correction.

Consequence of these issues is that an atmospheric correction may not work under all conditions with the same accuracy or may even totally fail under some conditions.

Another problem, which exists also for case 1 water, is sun glint, which may occur in more than half of a MERIS scene. MERIS as MODIS can not be tilted to avoid or reduce sun glint problems, as SeaWiFS is able to do. In coastal case 2 water sun glint may even superimpose the problem caused by high suspended matter and floating material. However, areas of the image with the risk of high sun glint, are flagged in MERIS images. It is recommended, at least if data of high quality are required, to exclude these areas from further processing. However, if it would be possible to determine the sun glint contribution and correct for it, a large portion of the images could be recovered for evaluation.

As described in the ATBD Atmospheric Correction for BEAM, part of these problems have been treated in the development of an atmospheric correction procedure for case 2 waters.

Thus, in this document we will report about the performance of this procedure for different scenes, in order to demonstrate the potential but also the limits.

4 Sun glint problem

Sun glint is caused by photons, which arrive at the sea surface without being scattered in the atmosphere and which are specularly reflected by the sea surface to the sensor, again without being scattered in the atmosphere on the way to the sensor. However, all photons, which are scattered only in the forward direction may also contribute to sun glint. With an absolute flat ocean, only the sun disc of about 0.5 degrees would be visible. In case of an imaging spectrometer ,such as MERIS, in form of a line in the image, which position depends on the orbit and solar angles. however, in nearly all cases the sea surface is rough even under calm conditions with ripple waves so that the theoretical line is broadened into a wide strip in that part of the image, which is directed to the sun. In case of MERIS and the orbit parameter of ENVISAT the right side of the image is always contaminated by sun glint. The breath of the strip depends on the waves slope distribution, which again depends on the wind speed.

Fig. 1: Sun glint as seen from a ship under calm conditions

Since at the time of overflight the wind speed may vary within the scene, it cannot be predicted from the mean wind as given in the auxiliary data of MERIS. The only way to determine the sun glint is from the signal itself.

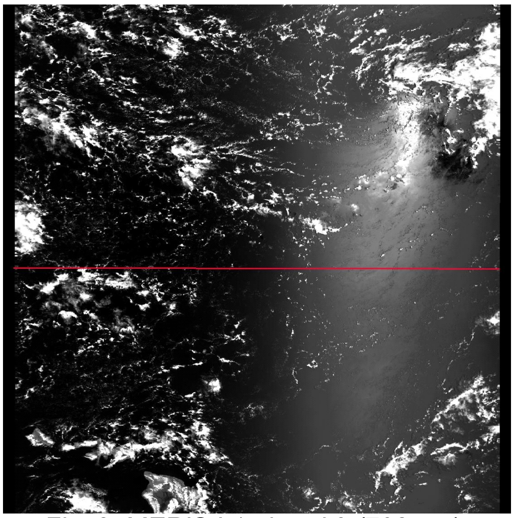

Fig. 2: MERIS L1, band 9 (708 nm), Hawaii 20030705

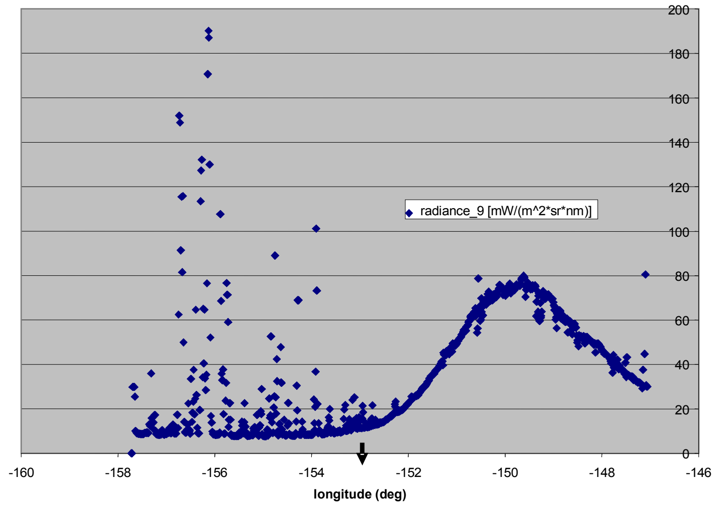

Fig. 3: Radiance distribution along the transect

Fig. 3 shows the nearly Gaussian shaped radiance distribution along the transect of Fig. 2. Sun glint starts already before the nadir as predicted by the model (s. below). The consequence is that half the image had to be flagged as sun glint contaminated (Fig. 4).

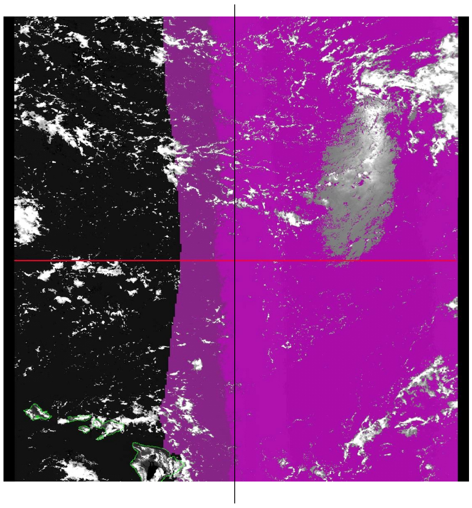

Fig. 4: As Fig. 2, but with flags for medium (deep purple) and high sun glint (bright purple), red line is the transect as seen in Fig. 3, vertical black line indicates the nadir

4.1 Simulation of the sun glint

For training of a neural network for atmospheric correction, which should include the sun glint, it was necessary to include sun glint photons. The Monte Carlo photon tracing model, we have developed and used for the radiative transfer simulations, allows to label photons according to the events they experience during their life in the model. For the purpose of analysing the contribution of sun glint photons to the path radiance, photons were labelled as sun glint as long as they did not experience a scattering event. These photons were counted separately from counting all other photons, which were scattered before they entered the detector.

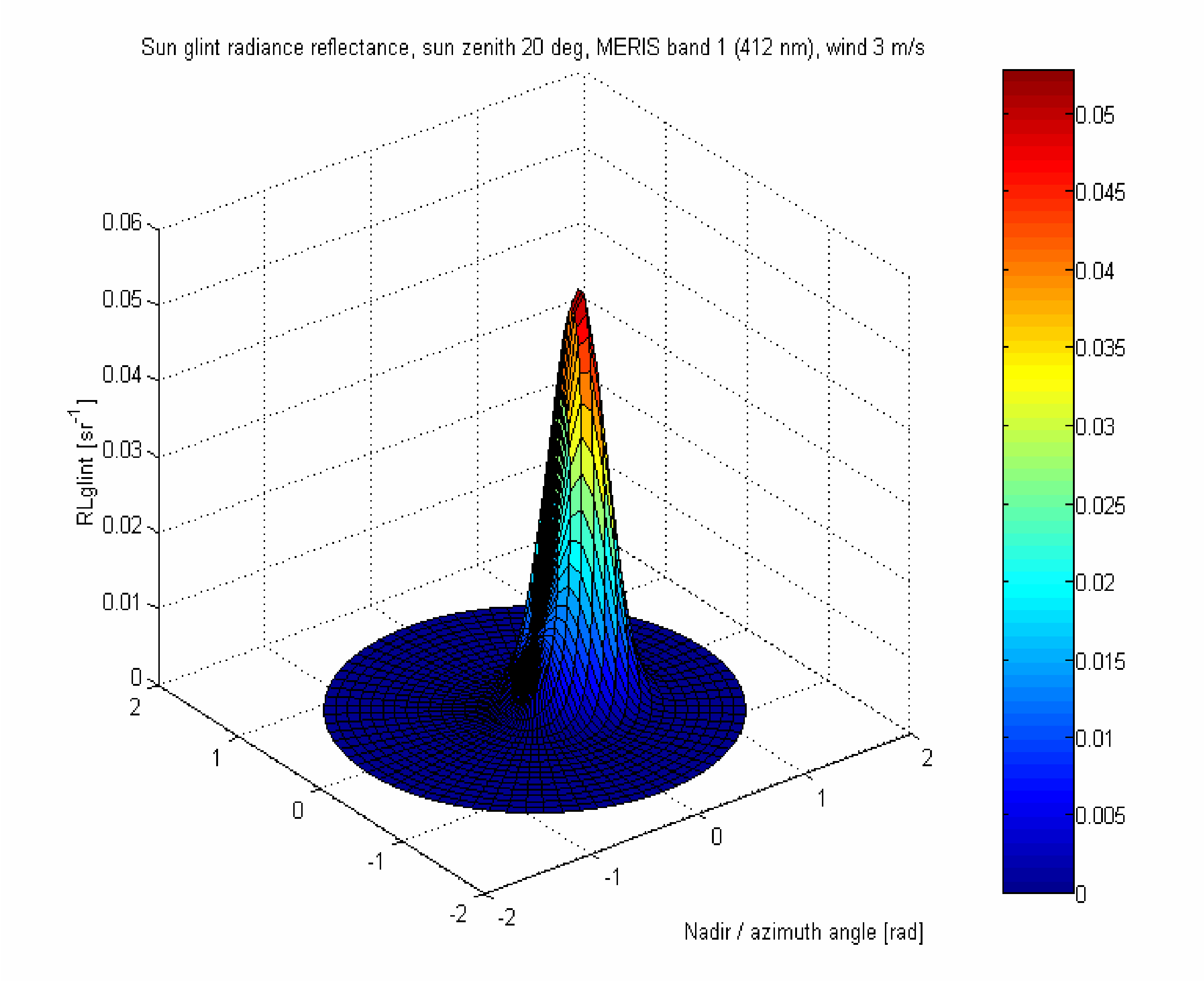

Fig. 5: Simulated radiance reflectance distribution of sun glint for a sun zenith angle of 20 deg. and a wind speed of 3 m/s

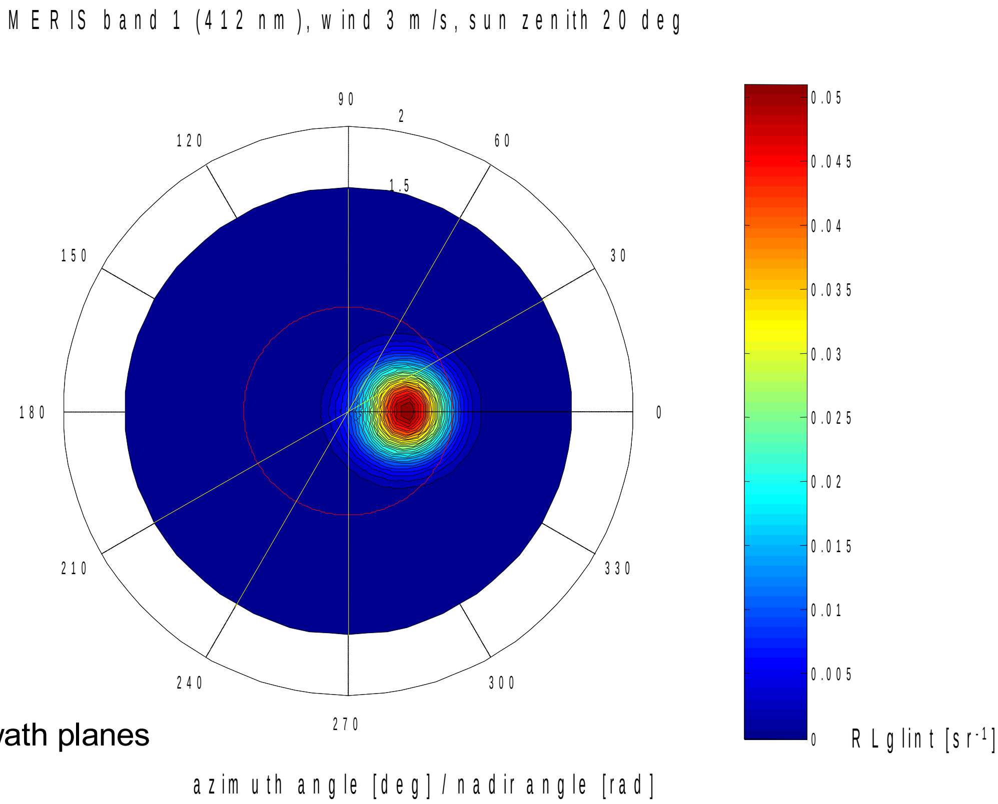

Fig. 6: Simulated sun glint radiance distribution with possible swath directions and circle of MERIS viewing zenith angle

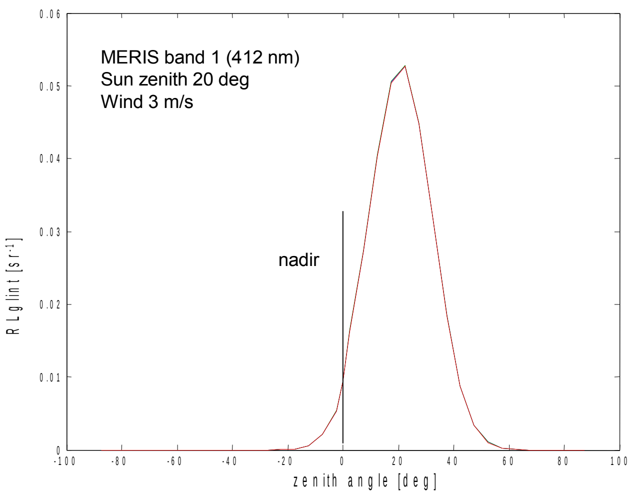

Fig. 7: Simulated sun glint radiance in solar azimuth plane

Very obvious from Fig. 6 and 7 is that for small sun zenith angles sun glint may be present also at nadir and even on the opposite side of the sun. These simulations are confirmed by the MERIS scene of Hawaii (s. Fig. 2 and 3). But also for medium sun zenith angles and higher wind speeds sun glint may reach the nadir, as shown in Fig. 8.

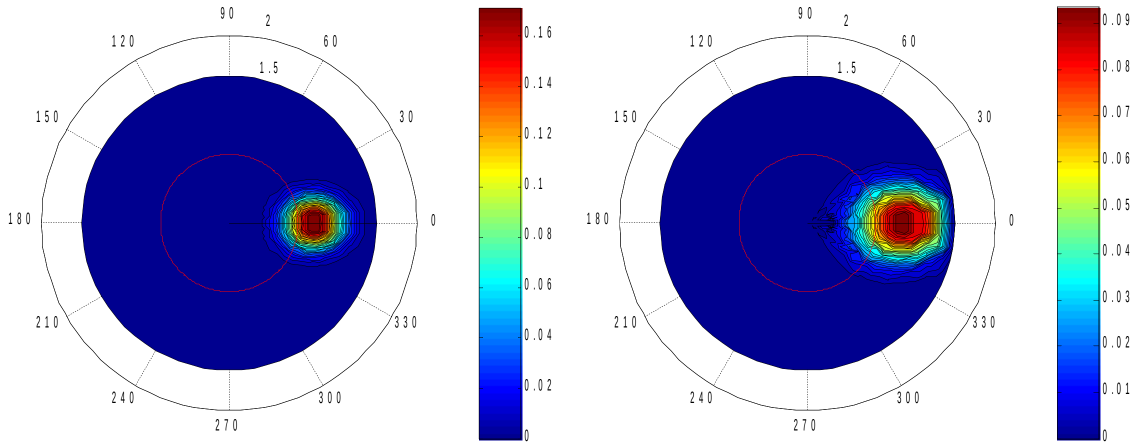

Sun 45 deg, wind 3 m/s

Sun 45 deg, wind 7 m/s

Fig. 8: Simulated sun glint distribution for sun zenith angle of 45 deg. and wind speeds of 3 m/s and 7 m/s

Another issue is the spectral distribution of sun glint as part of the path radiance, because the near infrared part is used for atmospheric correction, i.e. for extrapolating the path radiance to the blue spectral range. Since the overall path radiance (including Rayleigh scattering at air molecules) decreases with increasing wavelength, the contribution from sun glint becomes dominant. Consequence is that small errors in the determination of sun glint may cause large errors in extrapolation. Fig. 9 shows the simulated spectral distribution of sun glint and path radiance without sun glint.

The spectral distribution of sun glint can also be analysed by comparing TOA radiance spectra at top of atmosphere. Fig. 10 shows two positions along the transect in the Hawaii scene of 20030705 with a wind speed of 4-5 m/s. The two spectra at the positions inside and outside the sun glint are shown in Fig. 11, the ratio P1/P2 in Fig. 12. Obvious is the high sun glint contribution in the near infrared part, from which the atmospheric correction is performed.

This increase is also obvious in a scene of the Mediterranean Sea, spectra of which are shown at different positions inside and outside the sun glint in Figs. 13 and 14.

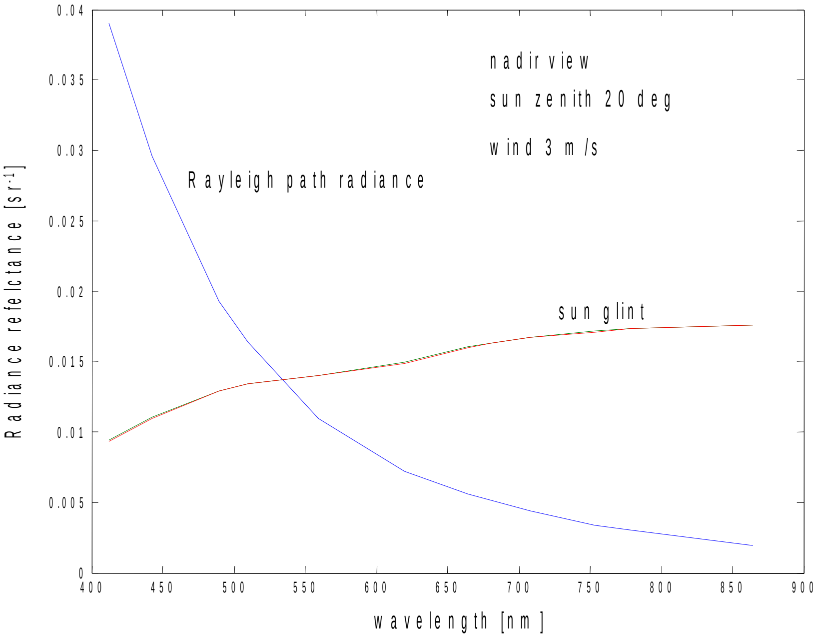

Fig. 9: Simulated radiance spectrum at top of atmosphere for only Rayleigh scattering and sun glint

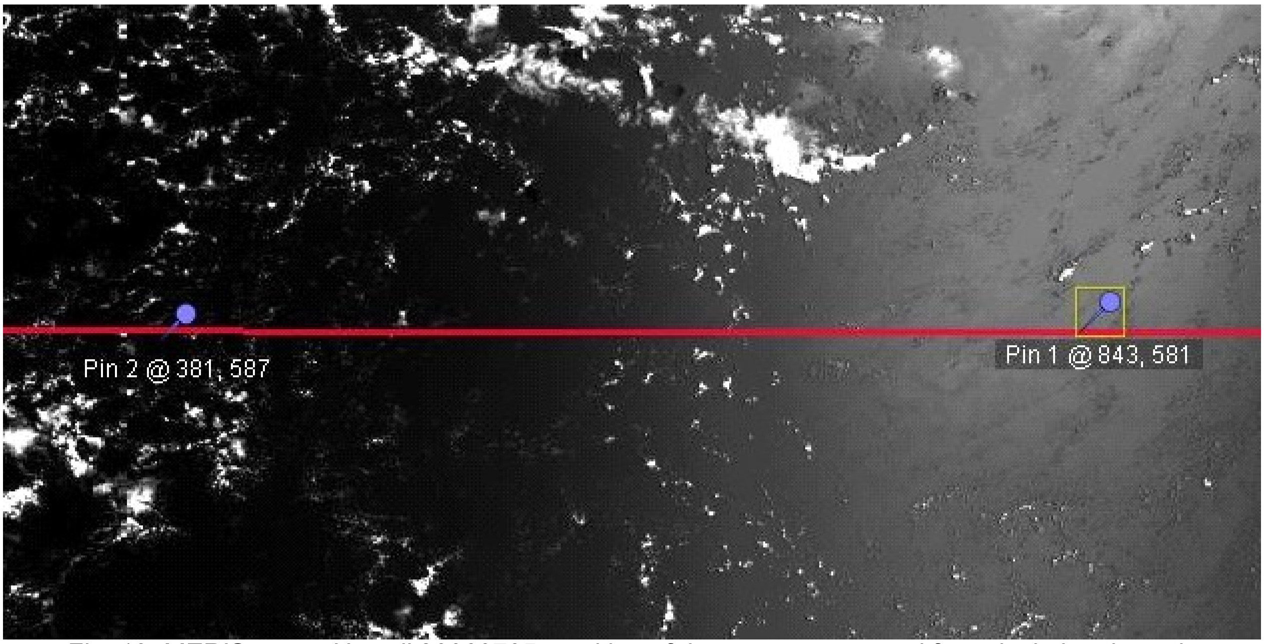

Fig. 10: MERIS scene Hawaii 20060705, position of the two spectra used for calculating the ratio

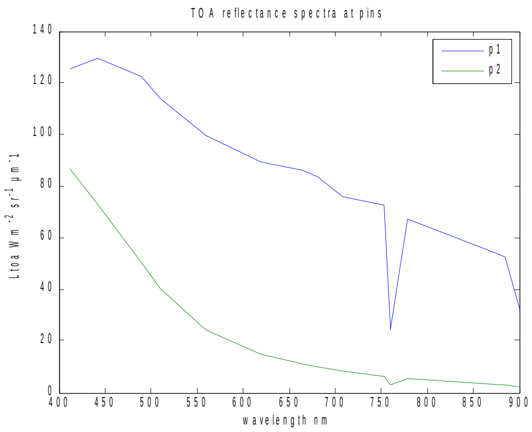

Fig. 11: Toa radiance spectra at position P1, inside, and P2, outside sun glint

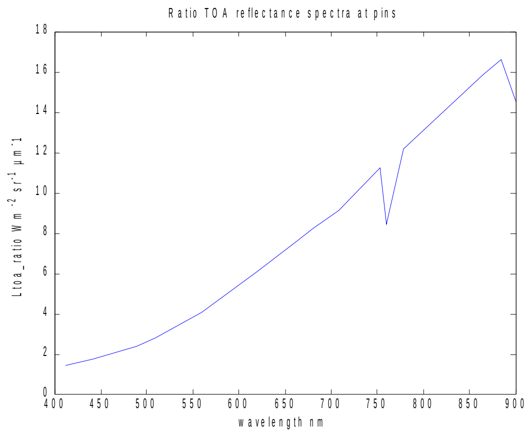

Fig. 12: Ratio between sun glint and non sun glint spectra (P1 / P2)

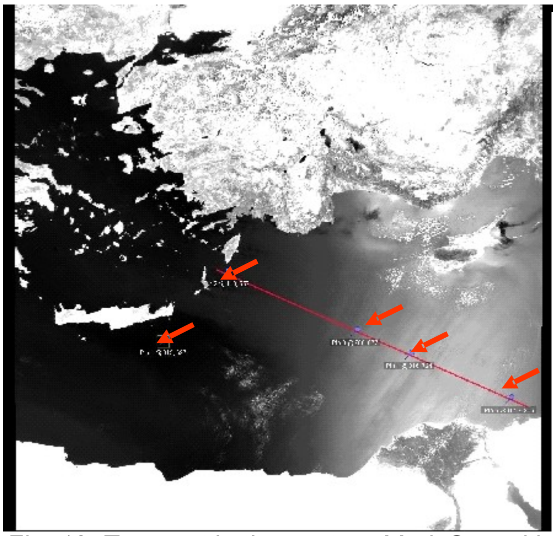

Fig. 13: Transect in the eastern Med. Sea with positions P1-P5 used for extracting the top of atmosphere radiance spectra

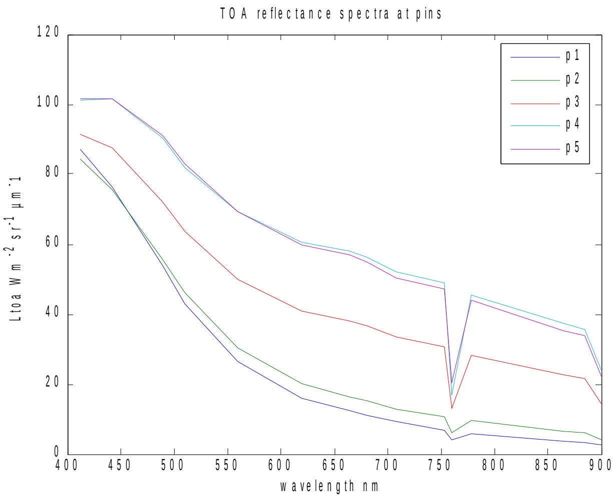

Fig. 14: TOA radiance spectra a the positions P1-P5 of the MERIS scene of the Med. Sea

4.2 Correction of the sun glint

The contribution by sun glint to the top of standard atmosphere radiance has been included in the simulations and, thus, in the training set for the neural network (NN), s. ATBD atmospheric correction. It was of interest to sea, if the NN can determine also strong sun glint at least over case 1 water. Thus, different scenes of the eastern Mediterranean Sea were used, where one can assume oligotrophic water and, thus, nearly constant water leaving radiance reflectances along a transect from outside to inside the sun glint.

Fig. 15 shows one of the scenes of 20020730 with the transect, which cuts the maximum of the sun glint, used to determine the different radiance components.

Fig. 16 shows the radiance reflectances for top of atmosphere, for the path radiance, which should include the sun glint, and for the water leaving radiance, which should not be influenced by the sun glint. It is obvious that the path radiance reflectance, as expected for the case of a successful sun glint correction, follows the TOA radiance reflectance, while the water leaving radiance reflectance remains more or less constant along the transect.

Furthermore, we have selected 3 positions along the transect and extracted the corresponding MERIS spectra. It can be seen that the RL_path together with RL_toa is increasing with increasing sun glint, while the RLw remains more or less uneffected.Small differences in RLw may also be due to a not constant water along the transect.

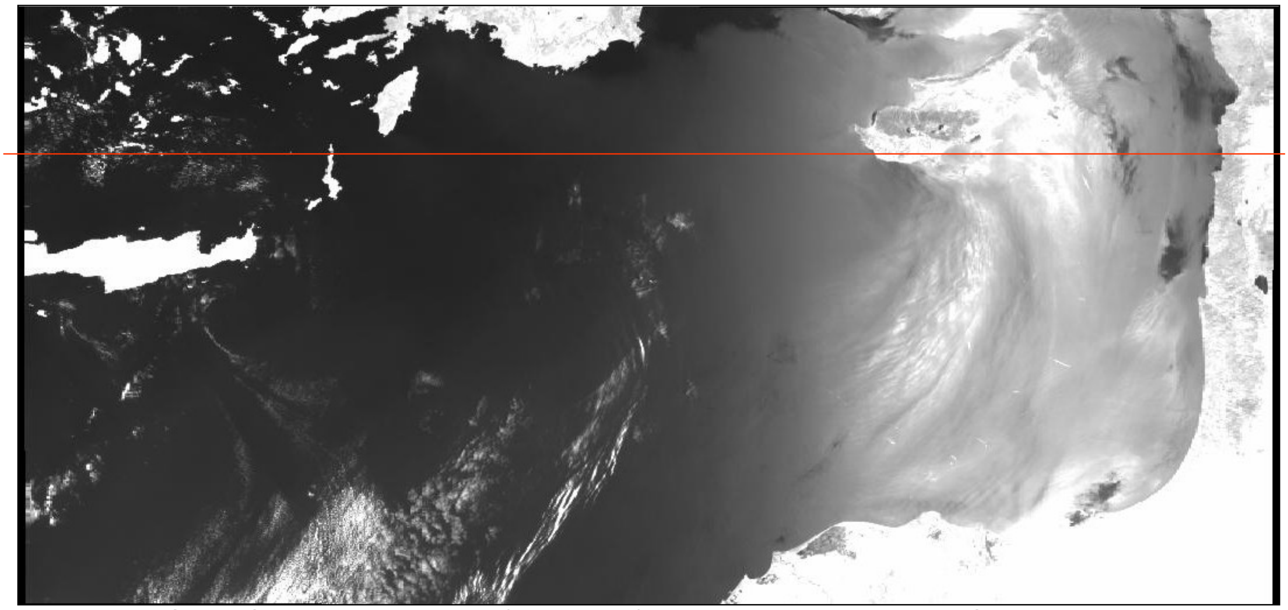

Fig. 15: MERIS L1 TOA radiance band 9 of a scene of the Eastern Mediterranean Sea with transect, 20020730

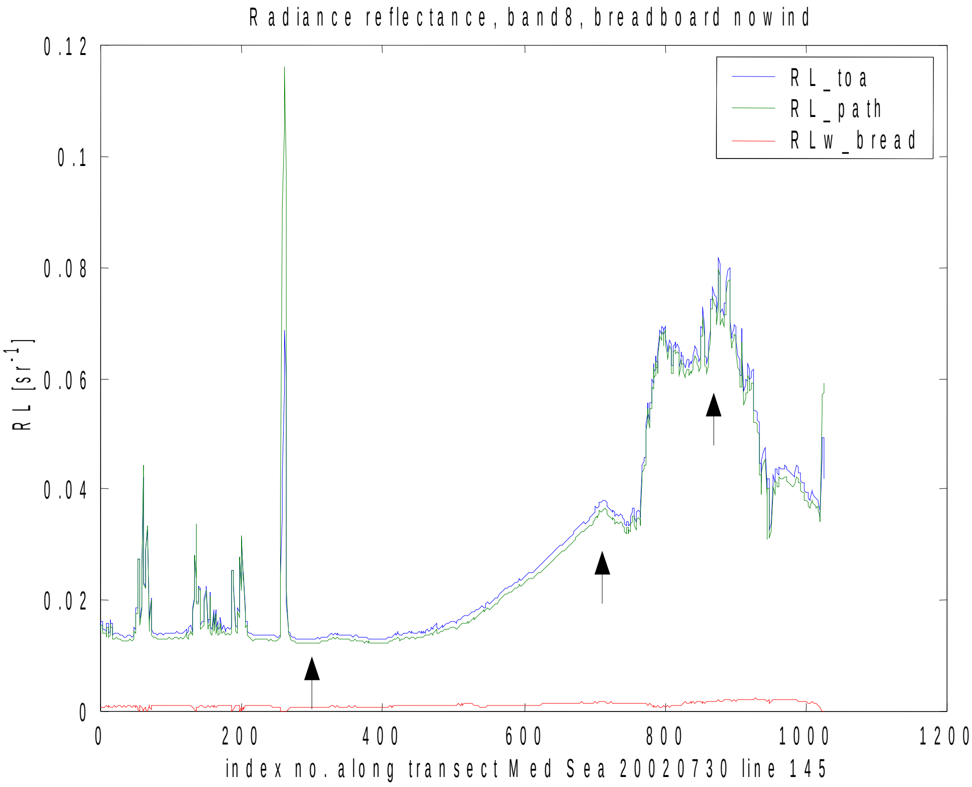

Fig. 16: Top of atmosphere RL_toa, path radiance RL_path and water leaving radiance RLw_bread along transect of MERIS scene of 20020730, arrows indicate positions of spectra outside in the middle and at maximum of sun glint

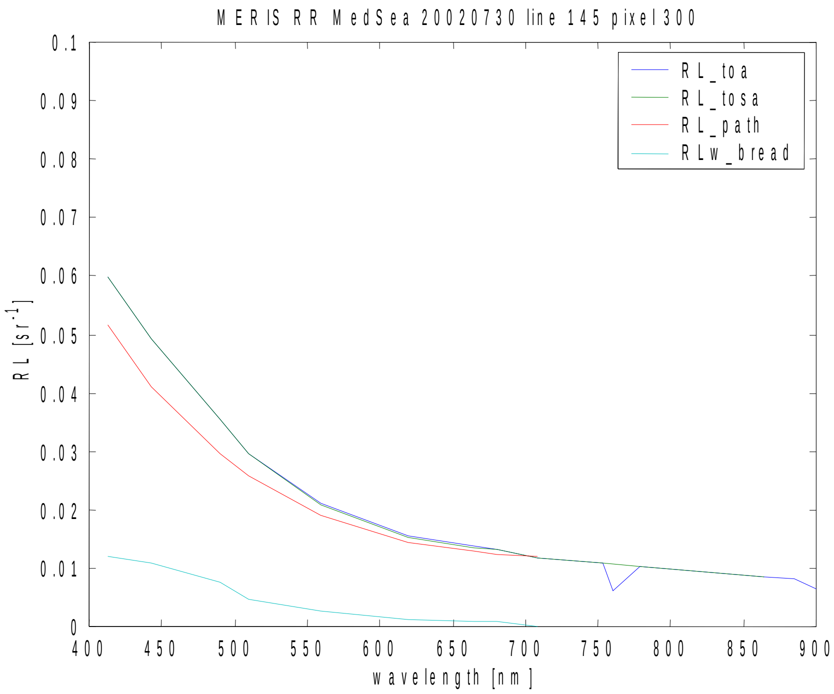

Fig. 17: MERIS spectra at transect position outside sun glint

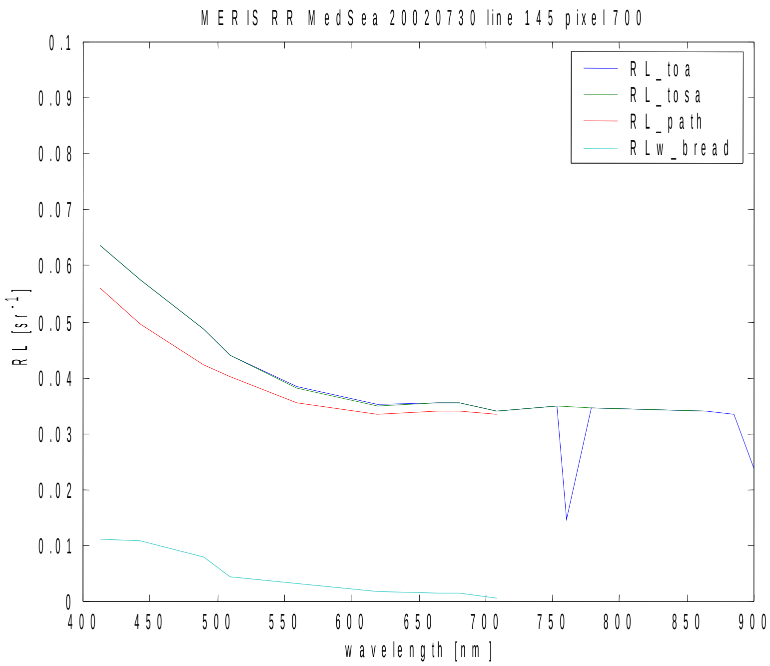

Fig. 18: MERIS spectra at transect position middle of sun glint

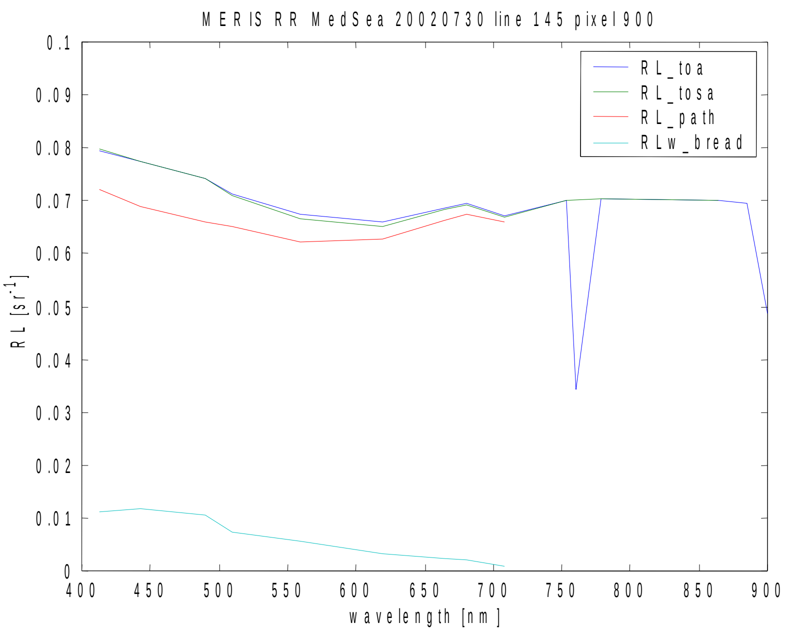

Fig. 19: MERIS spectra at transect position with maximum of sun glint

5 Conclusion

Sun glint imposes a severe issue for ocean colour sensors without a tilt mechanism, such as MERIS and MODIS. It can contaminate more than half of the image with the consequence of a much less revisit frequency than possible. The standard sun glint correction scheme, which is presently implemented in the MERIS ground segment processor, is based on a procedure which predicts the sun glint from the angles and the wind speed. Since the wind speed, as provided with the MERIS data, is not the wind at the time of overflight at a pixel, this procedure is not reliable.

In order to find a possibility to determine the contribution by sun glint to the top of atmosphere radiance and to find a correction scheme, we have included the sun glint into the Monte Carlo simulations and the training of the neural network for atmospheric correction.

First tests of different case 1 water scenes demonstrate that the sun glint can be determined from the radiance of the four MERIS NIR spectral bands at 708, 753, 778 and 865 nm. together with the solar and viewing zenith angle and the difference between the solar and viewing azimuth angle.

However, more cases have to be analysed to study the limit of this procedure, in particular for case 2 water conditions where high SPM concentrations, foam and other floating material contributes to the radiance of the four MERIS bands used for atmospheric correction.